

Trace Metals in Total Atmospheric Depositions (TAD) of a Nigerian Island

C.A. Onwudiegwu¹, G.C. Ezech^{2*}, I.B. Obioh²

¹African Institute for Science Policy and Innovations, Obafemi Awolowo University, Ile-Ife Nigeria

²Atmospheric Research and Information Analysis Laboratory (ARIAL), Centre for Energy Research and Development (CERD), Obafemi Awolowo University Ile-Ife

*Corresponding author: gcezeh@cerd.gov.ng, goddyich@yahoo.com

Abstract The paucity of data on air quality studies in Nigeria prompted us to commence the monitoring of total atmospheric deposition (TAD) in Lagos Island, Nigeria. TAD samples were collected every 30 days for a period of two years using a local assembled gauge fashioned after the Australian model gauge. Elemental characterization was carried out by Particle Induced X-ray Emission (PIXE) technique via an in-vacuum ion beam set-up. The TAD rates ranged from 1 to 62 g⁻¹m³month⁻¹. Twenty-eight elements (Na, Mg, Al, Si, P, S, Cl, K, Ca, Ti, V, Cr, Mn, Fe, Ni, Cu, Ga, As, Zn, Se, Br, Rb, Y, Nb, Mo, Sr, Zr and Pb) were detected in both fractions and their concentrations were assessed. Enrichment factors (EF) and pollution indices (PLI) were calculated and results revealed that most elements were anthropogenic with concentrations exceeding the World Health Organization guideline standards.

Keywords: atmospheric, anthropogenic, air quality, PIXE, pollution, ion beam

Cite This Article: C.A. Onwudiegwu, G.C. Ezech, and I.B. Obioh, "Trace Metals in Total Atmospheric Depositions (TAD) of a Nigerian Island." *Journal of Atmospheric Pollution*, vol. 4, no. 1 (2016): 15-22. doi: 10.12691/jap-4-1-2.

1. Introduction

In urban areas, anthropogenic activities have led to the generation of atmospheric emission of mostly sub-micron particles. These particles may be transported over very long distances: the so-called remote pollution by urban areas has been studied over lakes or seas where it may feature as a major trace metal input to large aquatic ecosystems. Nevertheless, significant wet and dry fallout also occur locally, and atmospheric fluxes onto impervious urban surfaces may significantly contribute to the contamination of urban runoff and play an important role in the urban cycle of metals, and further downstream on the contamination of receiving ecosystems. Although metal contamination of urban aerosols is widely recognized, only few studies [1,2,3,4] have been devoted to the Lagos conurbation. Yet the reported studies focused on size segregated aerosols (PM_{2.5} and PM_{2.5-10}) hence the need to investigate trace metals associated with TAD.

Metal transfer through the atmosphere is a significant part of the biogeochemical cycle of these elements [5]. There are two processes which increase heavy metal concentrations in the atmosphere: natural and anthropogenic [6]. Natural sources are mainly composed of soil, sea water and volcanic dusts and gases. Anthropogenic emissions come from industrial gases and aerosols or fossil-fuel combustion [7]. Incineration of urban waste is also identified as major atmospheric source of trace metals [8]. Metallic pollutants may be transported over long

distances as very small particles [9]. These particles when aggregated or washed out by rain are called atmospheric deposition, respectively, dry and wet. Dry deposition of particles occurs by direct impact and gravitational settling on land or water surfaces. In wet deposition, aerosols and gases are dissolved or suspended in water droplets or ice crystals. Besides such long-range transport processes, significant dry and wet depositions also occur locally, and atmospheric sources in urban area may play an important role in the metal contamination of atmospheric depositions [10]. Since heavy metals present high toxicity and high lability in atmospheric fallouts [11], its monitoring and characterization are important in-order to understand air quality issues that could arise in the environment due to elemental enrichments.

Accelerator-based ion beam analysis (IBA) techniques have been applied for characterization of heavy metals associated with TAD for many years [12]. They are well suited for such studies as IBA techniques have several unique advantages. The techniques have multi-elemental analysis capabilities; low minimum detection limits (MDLs) for a very broad range of elements in the Periodic Table and can quantitatively detect picograms of material in micrograms of sample [13]. With the use of IBA accelerator-based PIXE (Particle Induced X-ray Emission) technique, systematic investigations of TAD have been performed for several years [14]. Thus, with the application of IBA, an improved data set for source apportionment studies could be achieved since the output of source apportionment depends on the quality of elemental compositions analyzed [13].

2. Methodology

2.1. Description of Study Site

Lagos Island with coordinates (06° 27.276' N and 003° 23.256' E) was used for the study. It is high density traffic, commercial and low density residential area. The settlement pattern is poorly planned with closely clustered

elevated buildings; hence there could be high rate of environmental malpractices. The main economic activity in Lagos Island is commerce as it hosts two very big popular markets (Idumota and Balogun). No industry (metal smelting, beverage and conglomerates) exist within the neighbourhoods of Lagos Island, hence atmospheric emissions from the mainland with many industries could add to the TAD pollution loads within the receptor site.

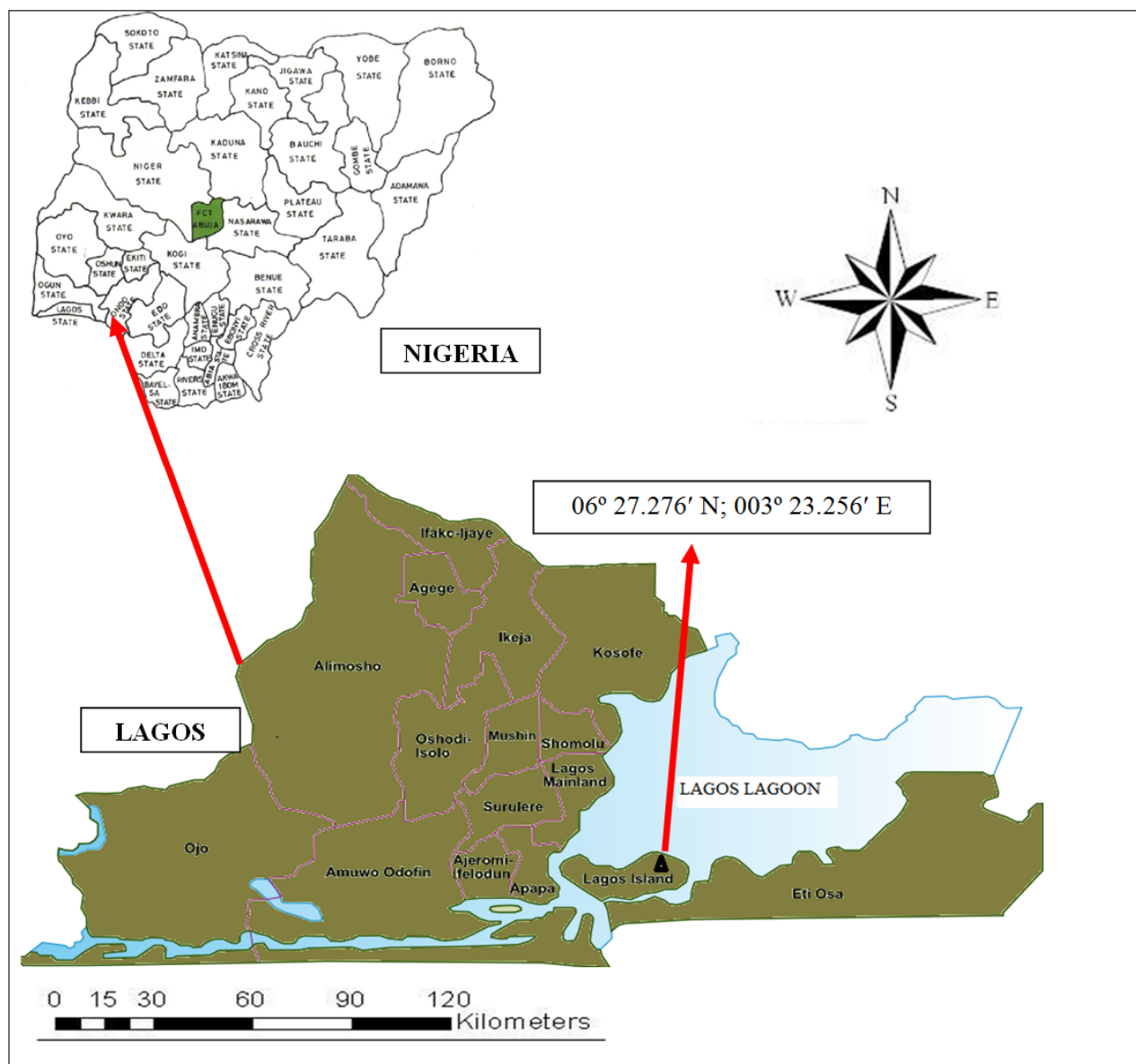


Figure 1. Map of the study site

2.2. Sampling

The sampling train (Figure 2) was assembled and placed on top of a 7-storey building (~25 m) high in-order to minimize the influence of entrained dust and hindrance of air motion. The sampling train which consists of locally assembled gauges fashioned after the Australian model gauge were installed stationary at the sampling point. The gauges are approximately 1.6 m and consist of a 14.50 mm diameter plastic funnel mounted on a plastic container housed in a metal casing of the gauge for support and stability. Harvesting of TAD samples was done every 30 days of exposure and the residue in the funnel was thoroughly washed into the plastic keg using de-ionized

water. The samples were labeled; TAD volumes were obtained using a measuring cylinder before and after filtrations through pre-conditioned and pre-weighed Whatman-42 cellulose ashless filter paper (thickness, 200 μm ; pore size, 2.5 μm and 125 mm diameter) via a filter assembly suction apparatus and deposition rates were calculated [15]. TAD samples were collected monthly for a period of two years and a total of forty-eight (48) samples were extracted and dried to constant weights at room temperature. Mass balance analysis of the samples were done using *Adventurer pro AV264* model weighing balance with sensitivity of 1 g prior to trace element analysis (via PIXE) and deposition rates were calculated [15].

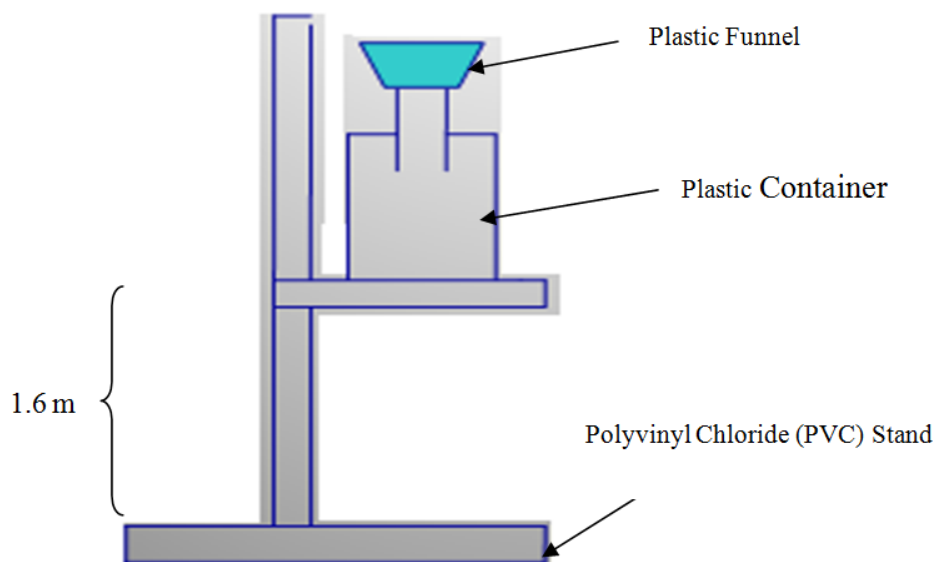


Figure 2. Schematic Diagram of a Locally assembled TAD Gauge

2.3. PIXE Measurements

For PIXE elemental analysis, 2.5 MeV proton beam with charge of $3 \mu\text{C}$ was irradiated on the samples. These samples were mounted on a ladder and positioned inside the target chamber at a distance of 1 cm from the window perpendicular to ion beam from the ion source. The chamber was kept in vacuum (10^{-7} Torr) and collimator 8 mm beam size was used in-order to cover large surface area on the filter during analysis. The target was positioned at 90° with respect to the beam direction and the characteristic X-rays were detected by liquid nitrogen cooled Si-Li detector (model ESLX 30 - 50, - 500 V) equipped with an $80 \mu\text{m}$ Kapton filter attached to the X-ray detector port. The detector signals were shaped and amplified through a pulse height analysis of the energy spectrum which was stored and displayed in a Canberra-88 model multi-channel analyzer. Each spectra acquisition time was 1200 seconds or 30,000 irradiation counts. Seven thin film IAEA certified standards were irradiated before starting irradiation of the aerosol samples in-order to calibrate the system and ensure reproducibility of the analytical facility. The quantitative analysis of the spectra obtained was carried out using the Analysis of X-ray spectrum by Iterative Least Squares fitting of GUPIX software [16], developed at Guelph University, Australia.

2.4. Data Analysis

2.4.1. Enrichment Factor (EF) and Pollution Indices (PLI)

To ascertain the extent of contributions of TADs to atmospheric elemental levels, enrichment factors (EF) were calculated for each element using crustal composition [17] with Ti as the normalizing element. The use of Ti as a normalizing agent is quite appropriate because it is a crustal element with less anthropogenic influence. Elements with EF next to unity have a strong natural component while elements with high EF could have anthropogenic origin, or are due to other natural sources such as marine aerosols. Pollution indices (PLI) of the elements were also used to assess the environment

quality and were calculated and classified as either low ($\text{PLI} < 1$), moderate ($1 \geq \text{PLI} \leq 3$) or high ($\text{PLI} > 3$) [18].

2.4.2. Pearson Correlation Matrix

The elemental concentrations of the analyzed TADs samples were also subjected to statistical analysis to determine the Pearson distance correlation matrix of the elements [19]. This was calculated using Statistical Package for Social Scientist (SPSS) software and correlation was considered significant at 0.05 levels (two tailed).

3. Results

3.1. TAD Rates

The average atmospheric deposition rates ($\text{g m}^{-3} \text{day}^{-1}$) obtained are presented in Figure 3. The lowest ($1 \text{ g m}^{-3} \text{day}^{-1}$) and highest ($62 \text{ g}^{-1} \text{ m}^3 \text{day}^{-1}$) deposition rates were recorded in September and February respectively. As expected, the concentrations recorded for Rain season months (April, May, June, July, August, September, and October) were found to be lower than TAD rates registered in the Dry season months (November, December, January, February and March). This could probably be due to differences in sampling times, for instance the scavenging of suspended atmospheric deposits is more pronounced in the Rain season while there could be minimal scavenging in the dry season (with no rainfalls). In addition, influence of seasonal Harmattan occasioned by the north-east trade wind with characteristic dust haze intensified dryness and extensive construction of buildings and urban infrastructure development could have contributed to the high levels TAD in Dry season months. In general, TAD rates were in most cases 10 times higher than values reported for industrial, rural and urban areas of Cantabria, Northern Spain [20] probably due to the influence of the Sahara dust which is more pronounced in Africa. High deposition rates represent the rates at which the observed elements are transferred to soils, water resources and vegetation [21].

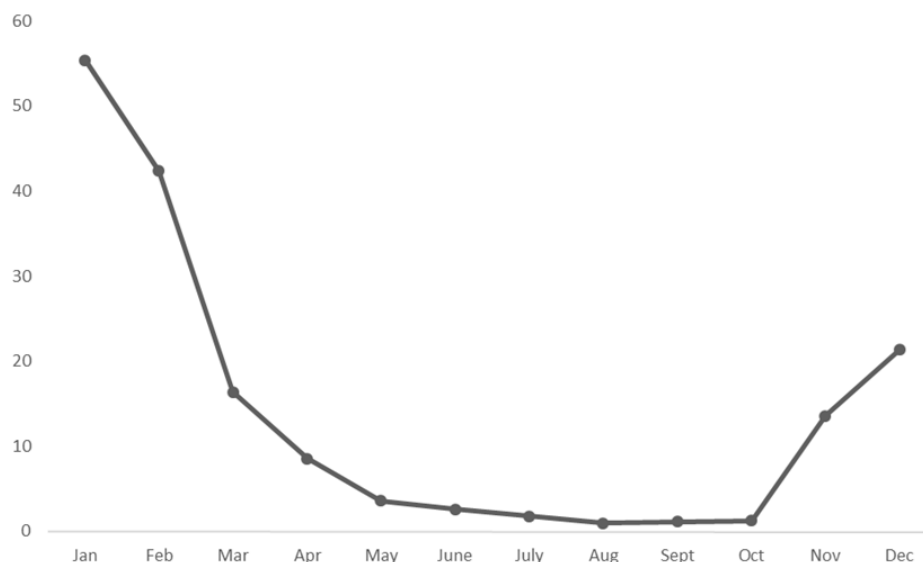


Figure 3. Average Total Atmospheric Deposition Rates

3.2. Multi-elemental Characterizations

Quality Assurance

The results of the International Atomic Energy Agency (IAEA) Certified Standard Reference for seven thin-film samples certified values are presented in Table 1 alongside with their corresponding laboratory-observed values and PIXE efficiency values. Generally, the PIXE facility results of the certified standards were above 95 % of the nominal values. Further attempt to validate the results showed that the standard variances of the experimental and theoretical data were < 2 for all the samples. This confirmed that the results were in agreement with certified values and it implies the reliability and reproducibility of the PIXE facility used for the analysis of the trace elements. Inadvertently, the uncertainty of concentration measurements varies from sample to sample and also from species to species. However, in atmospheric deposition

measurement the major source of uncertainty is not the concentration measurement, but in the method of collecting deposition samples [5]. For wet deposition, there may be some loss of the fine rain drops, especially under wind conditions. For dry deposition measurement, the funnel method has major uncertainties that are difficult to quantify and funnel walls present a significant aerodynamic interference to particle (and gaseous molecule) deposition. Particles, especially in the sub-micron to micron size range, are subject to Brownian, wind and turbulent eddy motion, and may be blown over and around the bucket or funnel walls rather than deposited into it. Once inside the funnel, the particles may adhere to the walls or deposit in the bottom of the collector. While we did rinse the collector walls with de-ionized water and filtered the solution for metals, the deposition area was taken only as the top area of the collector.

Table 1. Comparison of experimental and certified reference values

Thin films	IAEA Reference Standard ($\mu\text{g}/\text{cm}^2$)	Experimental values ($\mu\text{g}/\text{cm}^2$)	PIXE Efficiency (%)
Si	43.1	41.6	96.5
K	53.0	51.8	97.7
Ca	47.4	47.0	99.2
Fe	46.3	45.4	98.0
Ru	46.1	44.3	96.1
Pb	52.8	53.2	100.8
I	50.2	48.3	96.1

3.3. Trace Elements Fluxes, Enrichment Factors and Pollution Indices

Table 2 displayed the average trace metals fluxes, enrichment factors as well as pollution indices in the atmospheric deposition. Twenty-eight (28) elements (Na, Mg, Al, Si, P, S, Cl, K, Ca, Ti, V, Cr, Mn, Fe, Ni, Cu, Ga, As, Zn, Se, Br, Rb, Y, Nb, Mo, Sr, Zr and Pb) were detected by PIXE facility. TAD elemental fluxes contributed about 50 to 88 % of the overall mass loads deposited in the filter while the remaining percent could be attributed to unidentified low Z elements.

The highest average fluxes found for the metals were in the order; Fe ($115.356 \mu\text{g m}^{-3} \text{ day}^{-1}$) $>$ K ($63.476 \mu\text{g m}^{-3}$

day^{-1}) $>$ Ca ($43.324 \mu\text{g m}^{-3} \text{ day}^{-1}$) $>$ Si ($31.401 \mu\text{g m}^{-3} \text{ day}^{-1}$) $>$ Zn ($25.372 \mu\text{g m}^{-3} \text{ day}^{-1}$) $>$ Ti ($14.290 \mu\text{g m}^{-3} \text{ month}^{-1}$) $>$ Al ($5.277 \mu\text{g m}^{-3} \text{ month}^{-1}$). The high values recorded for the entrained dust markers (Ca, Al, Si, and Fe) could be explained because of their ubiquitous nature in the earth crust as well as the fact that the influence of dust could be prominent in Lagos where most road networks and walkways are unpaved and poorly maintained. Conversely, the origin of Al and Fe could also be linked to other sources such as ferrous and non-ferrous smelting industries. However, soil dust elements were not enriched and were also in low polluted class. Another prominent element is potassium whose origin could be attributed to soil dust, sea spray or biomass burning activities. Other elements

with significant concentrations are Na ($0.971 \mu\text{g m}^{-3} \text{ day}^{-1}$), S ($2.174 \mu\text{g m}^{-3} \text{ day}^{-1}$) and Cl ($1.8 \mu\text{g m}^{-3} \text{ day}^{-1}$). High concentrations registered for Na and Cl (marine sea-salt markers) is expected in Lagos air shed as our sampling point was located few kilometres away from the shores of the Atlantic Ocean. Inadvertently Na and Cl were not enriched in the TAD and also not classified as toxic metals though, persistent exposure could cause itching and discomfort. In addition, high PLI (13.64) recorded for Cl suggests anthropogenic influence.

Table 1. Trace elements mean concentrations, enrichment factors and pollution indices

	Mean (Error) ($\text{ng m}^{-3} \text{ day}^{-1}$)	**Typical Crustal Rock ($\mu\text{g g}^{-1}$)	EF	PIs
Na	971 (24)	23600	0.02	0.04
Mg	258 (8)	23300	0.00	0.01
Al	5277 (34)	82300	0.03	0.06
Si	31401 (123)	281500	0.04	0.11
P	795 (23)	nd	nd	nd
S	2174 (38)	260	3.34	8.36
Cl	1774 (53)	130	5.44	13.64
K	63476 (308)	20900	1.21	3.04
Ca	43324 (192)	41500	0.42	1.04
Ti	14290 (68)	5700	1.00	2.51
V	493 (19)	135	1.46	3.65
Cr	398 (11)	100	1.59	3.98
Mn	2454 (16)	950	1.03	2.58
Fe	115356 (115)	56300	0.82	2.05
Ni	108 (11)	75	0.57	1.44
Cu	577 (15)	55	4.18	10.48
Ga	91 (13)	nd	nd	nd
As	82 (19)	nd	nd	nd
Se	47 (13)	0.05	372.05	932.77
Zn	25372 (47)	70	144.57	362.45
Rb	555 (53)	90	2.46	6.17
Br	212 (21)	2.5	33.77	84.67
Y	218 (35)	nd	nd	nd
Zr	993 (53)	165	2.40	6.02
Nb	110 (33)	nd	nd	nd
Mo	178 (45)	nd	nd	nd
Sr	515 (34)	375	0.55	1.37
Pb	1156 (72)	12.5	36.90	92.51

** Adapted from Mason, (1966); "nd" means "not detected".

High Sulphur concentration ($2.174 \mu\text{g m}^{-3} \text{ day}^{-1}$) could be anthropogenic (energy production, biomass burning, refuse incineration or emissions from ships using heavy oil). Airborne sulphur rarely occurs as a pure element; it is usually produced as SO_2 gas which readily converts to sulphate SO_4^{2-} ions under normal atmospheric conditions.

The SO_4^{2-} ions can exist in the atmosphere as sulphuric acid producing acid rain and can either be partially neutralized to ammonium bisulphate or fully neutralized to ammonium sulphate [4]. Average Pb concentration ($1.156 \mu\text{g m}^{-3} \text{ month}^{-1}$) is 20 times higher than the World Health Organization [22] and the Europe guideline value (50 ng m^{-3}) for particulate matter. In addition, the high values of enrichment factor (36.90) and pollution index (92.51) registered for Pb is worrisome as Nigeria government has since 2003 placed a ban on the use of leaded gasoline. Therefore, high concentration of Pb in TAD of Lagos Island could be as a result of transport of

emissions from the smelting companies located in the hinterlands. Again, the mean concentrations of V ($493 \text{ ng m}^{-3} \text{ month}^{-1}$) and Ni ($108 \text{ ng m}^{-3} \text{ month}^{-1}$), the two markers for gasoline oil combustion emissions were also high compared to values for Spain [20]. This could be as a result of the growing number of automobile traffics as Lagos accounts for about 40 % percent of gasoline consumption in Nigeria. Total atmospheric Zn fluxes were surprisingly high in the study. The high concentration of this element was probably induced by leaching of building roofs which is made with Zn-covered metal sheets. The high EF and PLI values of Zn confirmed its anthropogenic origin. Indeed, we noticed that our TAD determination for Zn in Lagos Island is higher than previous works done in rural areas [23,24]. Such differences may be related to the presence of point sources, which are clearly site-specific. Other elements detected such as Cu, As, Cr, Se and Cs are known to be toxic; exposure even at low concentrations could pose adverse health effects on humans and animals [25]. Since no point sources are located in the vicinities of the studied rural area, the origin of metals could be attributed to medium to long-range transport from different sources. Thus, the residence time of these metals bound to particles in the atmosphere is much higher; indicating that rainwater dissolves these metals.

Due to the designation of sampling location as a coastal city, we estimated the contributions of the sea salt (ss) and non-sea salt (n-ss) components of Na, S, K and Ca respectively. Sodium can be directly emitted from the sea as sea spray and it is also present in crustal materials. The n-ssNa concentrations in the coarse and fine particulate fractions (TAD) were estimated using the crustal Na/Al ratio of 0.348 [26] as shown in equations 1 and 2, respectively:

$$n - ssNa = [Al] \times \left[\frac{Na}{Al} \right]_{CRUSTAL} \quad (1)$$

$$[Na]_{TOTAL} = ssNa + n - ssNa \quad (2)$$

where, the brackets denote measured concentrations.

Sulphur was one of the major elemental components measured by PIXE. Its origin could be mainly anthropogenic (as mentioned earlier). It can be directly emitted from fossil-fuel combustion processes and from sea spray however, it is mainly produced by SO_2 oxidation in the atmosphere. The n-ss S fluxes were estimated using the sea water S/Na ratio of 0.084 [13] as shown in equations 3 and 4 respectively:

$$ssS = [Na]_{ssNa} \times \left[\frac{S}{Na} \right]_{SEAWATER} \quad (3)$$

$$n - ssS = [S]_{TOTAL} - ssS \quad (4)$$

The sea-salt components of K and Ca, ssK and ssCa, were estimated using the generally accepted seawater K/Na (0.036) and Ca/Na (0.038) ratios [27] as shown in equations 5 and 6 respectively:

$$ssK = [Na]_{ssNa} \times \left[\frac{K}{Na} \right]_{SEAWATER} \quad (5)$$

$$ssCa = [Na]_{ssNa} \times \left[\frac{Ca}{Na} \right]_{SEAWATER} \quad (6)$$

Table 3. Sea salt (ss) and Non-sea salt (n-ss) of Na, S, K and Ca Components

Elements	Mean (Standard Deviation) (ng m ⁻³ day ⁻¹)
ssNa	768 (23)
n-ssNa	203 (1)
ssS	65 (2)
n-ssS	2110 (36)
ssK	28 (2)
n-ssK	63449 (306)
ssCa	29 (2)
n-ssCa	43295 (190)

As shown in Table 3, Na is mainly of marine origin (ssNa is about 80 % of total Na in the atmospheric deposits). Conversely, only a small fraction of S is due to sea salt; the n-ss components of S accounted for 97 % of total S. This could be an attestation that the bulk S origin was mostly anthropogenic probably from the hinterland with many industries. The n-ss component of K and Ca accounted for nearly 98 % of their total concentrations. However, we noted the disparity in the mean K/Na (65) and Ca/Na (45) ratios which also deviated from values reported elsewhere [27]. Several factors such as duration of exposure, season of sampling and aerodynamic size could be responsible for the high K/Na and Ca/Na ratios.

Table 4. Trace element correlation

	Na	Mg	Al	Si	P	S	Cl	K	Ca	Ti	V	Cr	Mn	Fe
Na	1.00													
Mg	0.88	1.00												
Al	0.33	0.57	1.00											
Si	-0.21	0.56	1.00	1.00										
P	-0.20	-0.61	0.68	-0.67	1.00									
S	0.59	0.27	-0.94	0.04	0.88	1.00								
Cl	0.94	0.95	-0.79	0.14	0.39	0.73	1.00							
K	0.80	0.91	0.96	0.28	0.86	0.89	0.91	1.00						
Ca	0.41	0.83	0.90	0.93	0.53	0.84	0.65	0.98	1.00					
Ti	0.20	-0.92	0.96	0.98	-0.56	-0.88	-0.92	1.00	0.98	1.00				
V	-0.91	-0.95	0.06	-0.96	-0.46	0.81	-0.85	0.27	0.91	0.97	1.00			
Cr	-0.80	-0.91	0.65	-0.97	-0.54	0.36	-0.03	0.19	0.98	1.00	0.77	1.00		
Mn	0.22	0.59	0.64	0.96	0.62	0.90	0.49	0.38	0.48	0.99	0.93	0.99	1.00	
Fe	0.24	0.91	0.94	0.96	0.26	0.32	-0.23	0.79	0.97	0.99	0.58	0.99	0.97	1.00
Ni	-0.98	0.21	0.09	-0.88	0.30	0.98	0.20	-0.87	0.79	-0.87	0.96	0.88	0.80	0.90
Cu	-0.81	0.08	0.90	0.33	0.40	0.37	0.15	0.45	0.95	0.28	0.27	0.98	0.96	0.99
Ga	0.44	0.04	0.88	-0.88	0.02	-0.81	-0.89	-0.92	0.91	0.62	-0.86	-0.90	0.92	0.91
As	0.06	0.23	0.23	0.29	0.80	0.95	0.72	0.39	0.51	-0.42	-0.29	0.43	0.50	0.44
Se	0.06	0.48	-0.56	0.57	0.95	0.79	0.33	0.48	0.47	0.48	-0.37	0.46	0.55	0.37
Zn	0.20	0.04	0.79	0.76	0.13	0.53	0.01	0.77	0.67	0.77	0.57	0.77	0.67	0.81
Rb	0.70	0.75	0.82	0.30	-0.54	-0.75	0.04	0.28	0.80	0.79	-0.74	-0.09	0.78	0.75
Br	0.86	0.87	0.24	0.26	0.27	0.79	0.85	0.85	0.85	0.88	0.83	-0.08	0.91	0.86
Y	0.24	-0.03	0.79	0.27	-0.33	-0.61	-0.66	-0.78	-0.77	-0.79	-0.82	-0.81	-0.77	-0.80
Zr	0.36	0.55	0.81	0.97	0.37	-0.61	-0.92	-0.76	0.85	0.98	0.68	0.20	0.84	0.78
Nb	0.62	-0.69	0.54	0.70	0.61	0.70	0.34	0.04	0.29	0.63	0.63	0.33	0.61	0.57
Mo	-0.55	-0.77	0.35	0.03	0.10	0.51	-0.58	0.57	0.15	0.74	0.84	0.13	0.63	0.78
Sr	0.46	0.57	0.84	0.85	0.29	-0.66	0.32	0.87	0.84	0.39	0.92	0.09	0.35	0.91
Pb	0.31	0.20	0.44	0.77	0.35	0.75	0.20	0.63	0.89	0.45	0.78	0.47	0.67	0.75

	Ni	Cu	Ga	As	Se	Zn	Rb	Br	Y	Zr	Nb	Mo	Sr	Pb
Na														
Mg														
Al														
Si														
P														
S														
Cl														
K														
Ca														
Ti														
V														
Cr														
Mn														
Fe														
Ni	1.00													
Cu		1.00												
Ga	0.88		1.00											
As	0.77	0.87		1.00										
Se	0.09	0.50	0.80		1.00									
Zn	0.21	0.34	-0.38	0.05		1.00								
Rb	0.96	0.78	0.71	0.06	-0.01		1.00							
Br	0.72	0.20	-0.12	0.20	0.41	0.57		1.00						
Y	0.71	0.87	0.39	0.60	0.48	0.63	0.77		1.00					
Zr	-0.86	-0.78	-0.70	0.20	-0.28	-0.82	-0.85	-0.80		1.00				
Nb	0.48	-0.83	0.07	0.78	0.41	0.32	0.35	0.76	0.50		1.00			
Mo	0.67	0.50	0.46	-0.22	0.56	0.58	0.07	0.58	-0.78	0.20		1.00		
Sr	0.92	0.75	0.22	-0.02	-0.04	0.15	-0.57	0.47	0.67	0.29	0.48		1.00	
Pb	0.89	-0.02	0.73	0.42	0.19	0.25	0.76	-0.89	0.86	0.67	0.59	0.73		1.00
	0.66	0.86	0.45	0.67	0.28	0.89	-0.10	0.91	0.78	0.33	0.22	0.07	0.08	1.00

Note: n = $\alpha = 0.001$, $r^2 \geq 0.248$ at 95 % Confidence Interval Level. Strongly correlated are shown in bold type.

3.4. Elemental Correlations (r^2)

The results of the Pearson elemental correlation matrices are presented in Table 4. The elements displayed both negative and positive correlations. For instance, Na correlated strongly with Mg ($r^2 = 0.88$), Cl ($r^2 = 0.94$), K ($r^2 = 0.80$) and Br ($r^2 = 0.86$) while it displayed negative correlations with V ($r^2 = -0.91$) and Cr ($r^2 = -0.80$) respectively. Similarly, Al has strong positive correlations with the soil dust markers Si ($r^2 = 1.00$), Ca ($r^2 = 0.90$), Ti ($r^2 = 0.96$), Fe ($r^2 = 0.94$), Sr ($r^2 = 0.84$) and Zr ($r^2 = 0.81$). Again, K displayed strong positive correlation ($r^2 = 0.89$) with sulphur while V and As showed negative correlation ($r^2 = -0.29$). Equally, the markers for industrial emissions (Zn and Pb) also displayed strong positive correlation ($r^2 = 0.89$). Thus, strong correlations found between the elements could indicate a common source or chemical similarity, whilst weak correlations could imply different source origin or non-chemical similarity [24].

4. Conclusion

During two years, atmospheric fallouts were collected monthly in Lagos Island in-order to assess the levels of atmospheric trace metals deposited over the area. The duration of the study was long enough to allow variations in fluxes of atmospheric depositions as well as for determination of temporal trends. A simple method of total atmospheric deposition collection using a locally assembled TAD gauge standing at 1.7 m above the ground within a PVC pipe was assessed. The average atmospheric deposition rates varied across the months; high values were recorded for the Dry season months (November, September, January, February and March) while the Rain season months (April, May, June, July, August, September, and October) recorded lower values. Twenty-eight (28) elements (Na, Mg, Al, Si, P, S, Cl, K, Ca, Ti, V, Cr, Mn, Fe, Ni, Cu, Ga, As, Zn, Se, Br, Rb, Y, Nb, Mo, Sr, Zr and Pb) as well as their concentrations were detected by PIXE technique. The elemental concentration of Pb were particularly high, exceeding World Health Organization's ambient tolerance limit factors ranging from 2 to 20 times. The health risk of Pb is very high and should be investigated regularly. We strongly recommend a national air quality monitoring network to determine daily TAD rates and associated elements in all Nigerian cities so as to improve on information regarding air quality database and consequently aid in development of local air quality guideline standards.

Acknowledgements

The authors are grateful to Professor's E.I Obiajunwa and D.A Pelemo as well as the entire accelerator staff team at Centre for Energy Research and Development (CERD) for their supports during PIXE experiment.

Disclosure Statement

No potential conflict of interest was reported by the authors.

References

- [1] Ezeh G.C., Obioh I.B., Asubiojo O.I. and Abiye O.E. (2012) PIXE characterization of PM₁₀ and PM_{2.5} particulates sizes collected in Ikoyi Lagos, Nigeria. *Journal of Toxicological and Environmental Chemistry*, 94(5), 884-894.
- [2] Obioh I.B., Ezeh G.C., Alfa A., Ojo E.O. and Ganiyu A.K., (2013) Atmospheric Particulate Matter in Nigerian Megacities, *Journal of Toxicological and Environmental Chemistry*, 95 (3), 379-385.
- [3] Ezeh G.C., Obioh I.B., Asubiojo O.I., Chiari M., Nava S., Calzolari G., Lucarelli F. and Nuviadenu C.K. (2014) Elemental Compositions of PM_{10-2.5} and PM_{2.5} Aerosols of a Nigerian Urban City using Ion Beam Analytical Techniques. *Nuclear Inst. and Methods in Physics Research*, B. 334, 28-33.
- [4] Ezeh G.C., Obioh I.B., Asubiojo O.I., Chiari M., Nava S., Calzolari G., Lucarelli F. and Nuviadenu C.K. (2015) The Complementarity of PIXE and PIGE Techniques: a Case Study of Size Segregated Airborne Particulates collected from a Nigeria City. *Journal of Applied Radiation and Isotopes* 103,
- [5] Azimi S., Ludwig A., Thevenot D.R., and Colin J-L. (2003) Trace metal determination in total atmospheric deposition in rural and urban areas. *The Science of the Total Environment* 308 (2003), 247-256.
- [6] D'Almeida GA, Koepke P, Shettle EP. Atmospheric aerosols: global climatology and radiative characteristics. A. Deepak publishing, 1991. (561 pp).
- [7] Pacyna JM. Estimation of the atmospheric emissions of trace elements from anthropogenic sources in Europe. *Atmos Environ* 1984;18(1):41-50.
- [8] Sullivan R, Woods I. Using emission factors to characterise heavy metal emissions from sewage sludge incinerators in Australia. *Atmos Environ* 2000;34: 4571-4577.
- [9] Koutrakis P. Physico-chimie de l'aerosol urbain: identification et quantification des principales sources par analyse multivariable. Atmospheric Environment Ph.D. University Paris XII-Val de Marne, 1984. (143 pp).
- [10] Mijic Z., Stojic A., Perisic M., Rajsic S., Tasic M., Radenkovic M. and Joksic J., Seasonal variability and source apportionment of metals in the atmospheric deposition in Belgrade. *Atmospheric Environment*, 44, 3630-3637, 2010.
- [11] Golomb D, Ryan D, Eby N, Underhill J, Zemba S. Atmospheric deposition of toxic onto Massachusetts Bay-I. Metals. *Atmos Environ* 1997;31(9):1349-1359.
- [12] Cohen, D.D.; Stelcer, E.; Santos, F.L.; Prior, M.; Thompson, C. and Pabroa, P.C.B. 2008. Fingerprinting and source apportionment of fine particle pollution in Manila by IBA and PMF techniques: A 7-year study. *X-ray Spectrometry*.
- [13] Cohen DD, Garton D, Stelcer E, Hawas O, Wang T, Poon S, Kim J, Cheol-Choi B, Nam-Oh S, Hye-Jung S, Ko MY, Uematsu M (2004) Multi-elemental analysis and characterization of fine aerosols at several key ACE-Asia sites. *Jour of Geophys Res* 109: D19S12.
- [14] Calzolari G., Chiari M., Lucarelli F., Nava S. and Portarena S. (2010) Proton induced γ -ray Emission Yields for the Analysis of Light Elements in Aerosol Samples in an External Beam Set-up. *Nuclear Instruments and Methods in Physics Research B* 268, 1540-1545.
- [15] Akeredolu F.A. (1989) Seasonal Variation in Deposition Rates, Concentration and Chemical Composition of Particulate Matter in Ile-Ife, Nigeria. *Atmos. Environ.*, 23, 783.
- [16] Maxwell JA, Teesdale WJ, Campbell JL, Nejeddy Z, (1995) The Guelph PIXE software package II. *Nuc Inst and Methods in Phy Res (B)* 43: pp. 395-407.
- [17] Taylor, S.R., 1964. Abundance of Chemical Elements in the Continental Crust; A New Table. *Geochimica et Cosmochimica Acta*, 28(8), 1273-1285.
- [18] dos Anjos MJ, Lopes RT, De Jesus EFO, Assis JT, Cesareo R, Barradas CAA (2000) Quantitative analysis of metals in soil using X-ray fluorescence. *Spectrochim. Acta (B)* 55: 1189-1194.
- [19] Sze kely, G.J., Rizzo, M.L., Bakirov, N.K. 2007. Measuring and testing independence by correlation of distances. *Annals of Statistics* 35/6, 2769-2794.
- [20] Puente M., Fernández-Olmo I. and Irabien A. (2013) Variability in metal deposition among industrial, rural and urban areas in the Cantabria Region (Northern Spain) *WIT Transactions on Ecology and The Environment*, 174.

- [21] Oluwole A.F., Olaniyi H.B., Akeredolu F.A., Ogunsola O.J., Asubiojo I.O (1988) Determination of the Environmental Impact in the Area of Operation of WAPCO, Consultancy. Services Centre, Obafemi Awolowo University, Ile-Ife.
- [22] World Health Organization, (2003) Report on a WHO Working Group, EUR/03/504268.
- [23] Migon C, Journel B, Nicolas E. Measurement of trace metal wet, dry and total atmospheric fluxes over the Ligurian Sea. *Atmos Environ* 1997; 31(6): 889-896.
- [24] Ridame C, Guieu C, Loye-Pilot M-D. Trend in total atmospheric deposition fluxes of aluminium, iron, and trace metals in the northwestern Mediterranean over the past decade (1985–1997). *J. Geophys Res* 1999; 104(D232): 30127-30138.
- [25] World Health Organization (2006) Air quality guidelines for particulate matter, ozone, nitrogen dioxide and sulfur dioxide global update. World Health Organization (WHO) Geneva Switzerland.
- [26] Mason B (1966) Principles of geochemistry. Third ed., Wiley: New York
- [27] Weast, R.C. and Astle, M.J., 1982. Handbook of Chemistry and Physics, CRC Press, Boca Raton Fla.